Journal of
Ceramic Science
and Technology

*J. Ceram. Sci. Technol.*, **08** [4] 505-512 (2017)
DOI: 10.4416/JCST2017-00029
available online at: http://www.ceramic-science.com


# Tricalcium Phosphate Nanostructures Loaded with Bisphosphonate as Potential Anticancer Agents

**M. Rahmanian[1], S.M. Naghib[*2], A. Seyfoori[1], A.A. Zare[1, 3], K. Majidzadeh-A[1, 4], L. Farahmand[1, 3]**

[1]Biomaterials and Tissue Engineering Department, Breast Cancer Research Center, Motamed Cancer Institute, ACECR, Tehran, Iran.
[2]Nanobioengineering Division, Nanotechnology Department, School of New Technologies, Iran University of Science and Technology (IUST), P.O. Box 16846 – 13114, Tehran, Iran.
[3]Recombinant Proteins Department, Breast Cancer Research Center, Motamed Cancer Institut, ACECR, Tehran, Iran
[4]Genetics Department, Breast Cancer Research Center, Motamed Cancer Institut, ACECR, Tehran, Iran
received April 30, 2017; received in revised form June 25, 2017; accepted July 15, 2017

**Abstract**

**Nanostructured calcium phosphate carriers are emerging as a bisphosphonate delivery system that has demonstrated inhibitory effects in preventing bone metastasis, thereby improving the treatment of breast cancer. In this research, the inhibitory effect of loaded zoledronic acid (ZA) in tricalcium phosphate nanostructures (TCPNs) synthesized with the co-precipitation method was investigated. The results of microstructural analysis indicated that the sintering temperature has a slight influence on the synthesized crystallite size. The sintered crystallite size of tricalcium phosphate (TCP) at 800 °C (β-TCP) and 1450 °C (α-TCP) was calculated to be in the nanoscale range. The inhibitory effect of TCPNs (with different phases) on cancer cell lines including MCF-7 (breast cancer) and G-292 (osteosarcoma cancer) was investigated. *In vitro* results confirmed that the TCPNs were able to inhibit the proliferation of breast cancer cells. Experimental results of MCF-7 cell culture after two days proved that the growth of the cancer cells was inhibited by about 61 % and 83 % after treatment with β-TCP and α-TCP, respectively. Bisphosphonate-loaded TCPNs had no toxicity according to MTT assay results, but did have an inhibitory effect on MCF-7 cancer cells. The time dependence of ZA drug release from α and β-TCP and its effect on MCF-7 and G-292 cell treatment was investigated. The results suggested that TCPNs are promising materials that could be developed for treating local bone and breast cancers.**

*Keywords: MCF-7, G-292, tricalcium phosphate, nanomedicine, inhibitory effect*

## I. Introduction

It is known that bone is the primary site for breast cancer metastasis, a disease that can progress to fracture, spinal cord compression, hypercalcemia, pain, and a devastating decrease in the quality of life [1]. The aptitude of breast cancer metastasis to bone presumably represents some complicated communication between the metastatic bone, cancer cells, and the intermediary positional microenvironment [2]. Loaded bisphosphonate carriers have greatly ameliorated the systemic treatment of advanced breast cancer by decreasing the frequency and morbidity of skeletal-related events [3]. In recent years, many researchers have approved synthetic TCPNs in orthopedic applications owing to their biocompatibility, excellent bioactivity, adequate biodegradability, high affinity to polymers, biomacromolecules and high osteogenic potential [4–8]. Peng *et al.* reported that TCPNs could enhance the growth of bone cells based on an osteoconduction mechanism without causing any local or systemic toxicity, inflammation or foreign body response [9]. Also, in comparison with microscale TCP, nanostructured TCP has unique characteristics such as improved hardness and fracture, rectified bone bonding properties, promoted drug loading capacity and enhanced solubility [10].

In previous reports, ZA was known as a potent nitrogen-containing bisphosphonate that inhibited osteoclastic bone resorption and was permitted for the treatment of bone metastasis [11]. It was proven that the ZA antitumor effect comes from its inhibition of tumor cell proliferation, apoptosis induction, angiogenesis inhibition and diminution of tumor cell adhesion, invasion, and migration. The evidence of clinical trials indicated that ZA ameliorated long-term survival of cancer patients with and without bone metastasis [12]. Among the various synthetic biomaterials used for reconstruction of the target site in bone tissue, it is clear that calcium phosphate ceramics containing hydroxyapatite (HA) and TCP are considered as the most biocompatible and osteoconductive drug carriers for clinical bone drug delivery [13]. Forasmuch as the chemical composition of calcium phosphate ceramics is intimately similar to bone, such biomaterials could be resorbed again *in vivo* by cells and eventually promote bone formation [14].

* Corresponding author: naghib@iust.ac.ir

In recent decades, different researchers have demonstrated the inhibitory effect of ZA on breast cancer cells [15, 16].

The inhibitory effect of nanostructured hydroxyapatite (nHAP) on cancer cell proliferation was first proposed in the 1990s and led to great interest in nanotechnology and applied medicine fields, opening a new window for future researchers. Meena *et al.* [17] observed that nHAP inhibited the proliferation of breast cancer cell line MCF-7, he also found that these nanoparticles had a stronger anti-cancerous effect than macro or micro ones. The cell proliferation inhibition rate was dramatically increased in a concentration-dependent behavior of nHAP. This study showed a large increase in reactive oxygen species (ROS) in nHAP-treated cancer cells as well as that nHAP could induce p53 activities, which may be responsible for DNA damage and cell apoptosis [18]. In other similar research, Han *et al.* [18] proposed that nHAP possessed excellent ability in inhibiting some cancer cell proliferation such as MGC-803, Os-732, and Bel-7402 *in vitro* and *in vivo*. *In vitro* investigations of dose-dependent nHAP-treatment demonstrated that human cancer cell proliferation was inhibited by more than 65 % followed by less than 30 % for human normal cells. Moreover, *in vivo* studies exhibited that nHAP injection in a transplanted tumor led to a considerable reduction in tumor size (about 50 %). These results clearly showed that nHAP as a calcium phosphate could inhibit cancer cell proliferation and has high potential for biomedical application in cancer treatment. Inhibitory effects of other components of calcium phosphate can be interesting for future research owing to their biological characteristics and anticancer properties.

In this research, for the first time, the anticancer effects of TCPNs in different phases, as a new material which can be loaded with and without ZA drug was investigated *in vitro* on the growth of some cancer cells. The main structural characteristics of TCPNs were determined in XRD, FTIR, and SEM analysis. The different inhibitory effects of TCPNs on the proliferation rate of MCF-7 and G-292 cancer cell lines with consideration of the influence of the TCPN concentration (in eight doses from 50 to 600 mg/L) were studied *in vitro* in order to find an optimized state for the best treatment. This manuscript can be regarded as a primer on the introduction of TCPNs loaded with ZA into the treatment of different cancer cells so as to encourage researchers to undertake more work in this field in the future.

## II. Materials and Methods

### *(1) Materials*

Calcium nitrate tetrahydrate ($Ca(NO_3)_2{\cdot}4H_2O$, 99.95 %), diammonium hydrogen phosphate ($(NH_4)_2HPO_4$, 99 %), sodium hydroxide (NaOH, 99 %), and ammonia solution ($NH_3$) were purchased from Merck Co. (Germany). Materials handling, storage, use, and disposal were performed according to the 29CFR 1926.250 standard.

### *(2) Synthesis of Nanostructured β-TCP and α-TCP powder*

The co-precipitation method for producing α-TCP [19] and β-TCP [20] was described in previous works. In this research, α and β-TCP nanopowders were synthesized with this method. To obtain a homogenous solution, 0.4 mol $(NH_4)_2HPO_4$ solution with pH 11 was stirred at room temperature, and 0.6 mol $(Ca(NO_3)_2{\cdot}4H_2O)$ with the same pH was dropped approximately with a rate of 15 – 20 mL/min to achieve a white precipitate. The ammonia solution was used to keep the pH of the system in the range of 10 – 12 and obtain a white precipitate with high homogeneity. It was recommended that the ammonia solution should be stirred at room temperature for 15 h. After the precipitate had been washed with distilled water, it was dried at 80 °C for 24 h and then calcined at 800 °C for 2 h to obtain β-TCP and the same process with calcining at 1450 °C for 5 h was applied to synthesize α-TCP.

### *(3) Materials characterization*

To determine the type of the TCPNs and their chemical bonds, FTIR (Shimadzu, 8400S, Japan) was utilized at the wavelength range of 300 – 4500 $cm^{-1}$. Formation of the TCP phase was evaluated based on the XRD pattern using a Siemens-Bruker D5000 system (Germany). The XRD diagrams were obtained for $4° \leq 2\theta \leq 70°$ angles with Cu Kα radiation (1.540 Å). In order to investigate the morphology and structural evolution of TCP nanopowders, SEM observations were performed with the VEGA-TESCAN system, USA. The SEM samples were prepared by adding 0.5 g of TCP nanopowders to 30 mL ethanol and applying ultrasound for 2 min. Then, for final preparation, one drop of the solution was placed on glass and dried at room temperature for 24 h.

### *(4) Preparation of TCP/ZA NPs complex*

The TCPNs were dispersed and mixed in an aqueous solution like phosphate buffer solution at pH 9.5 with ZA concentration of 0.08 g/L to achieve TCP/ZA complex.

### *(5) UV-Vis spectra analysis*

The *in vitro* release of bisphosphonate from the nanostructures was carried out in a closed 15-mL polypropylene flask. The weighed nanostructures were kept in 10 mL PBS (pH 7.4). The flasks were shaken at 37 °C in a precision reciprocal shaking water bath at 80 rpm. For further evaluation, 10 mL of the release medium was collected at regular time intervals (1, 12, 24 h, 2 and 7 d) and replaced with 10 mL fresh buffer. *In vitro* release studies were performed three times for each specimen. Finally, the bisphosphonate content in the release medium was determined by means of UV spectroscopy.

### *(6) Cell culture*

MCF-7 and G-292 cells were cultured in a 25-$cm^2$ flask in a medium containing Dulbecco's Modified Eagle's Medium (DMEM/Gibco), 10 % FBS, 100 U/mL penicillin, and 100 μg/mL streptomycin at 37 °C with 5 % $CO_2$, 95 % air, and complete humidity. Once they reached ~ 90 % confluency, they were detached using 0.05 % trypsin/EDTA and counted by means of trypan blue and hemocytometer. These cells were then resuspended at a concentration of $1 \times 10^5$ cells and added onto a 96-well plate. After 24 h, when the cells were adjacent to the plate bottom, the culture media were replaced with treatment media. All treatment media contained 90 % culture medium, 10 % FBS,

and different amounts of TCPNs at the final concentrations, which were 50, 100, 150, 200, 300, 400, 500 and 600 mg/mL, respectively. The proliferation of human cancer cell lines in the presence or absence of ZA loaded by TCPNs was determined by means of MTT assay.

### *(7) MTT assay for evaluating cell viability*

In order to evaluate the cell viability, after 48 h, the MTT solution was prepared at 1 mg/mL concentration in PBS and passed through a 0.2-μm filter. Then, 22 μL MTT plus 200 μL DMEM were added to each well, except for the cell-free blank wells. The cells were incubated for 4 h at 37 °C with 5 % $CO_2$, 95 % air, and complete humidity. After 4 h, the MTT solution was removed and replaced with 100 μL DMSO. The plate was further incubated for 15 minutes at room temperature, and the optical density (OD) of the wells was determined with a plate reader (Biotek) at 570 nm wavelength, the reference wavelength was, however, 630 nm.

## III. Results

Nowadays, it is clear that evaluating the morphology and microstructures of materials and biospecies with biological properties is a key concept in the characterization of biomaterials. In this regard, the morphology of the deposited TCPN powder is shown in Fig. 1(a) and (b) for α and β-TCP, respectively. Fig. 1(c) shows the FTIR spectrums of the TCP polymorphs powders formed at 800 °C for 2 h (β-TCP) and 1450 °C for 5 h (α-TCP).

The inhibitory influences of TCPNs on the MCF-7 cancer cell line proliferation were evaluated at different concentrations in the range of 50 to 600 mg/L. The results are shown in Fig. 2, which shows that TCPNs can inhibit the proliferation of human breast cancer cells. Over the last decade, TCPNs have been widely used as a biocompatible material for bone replacement and tissue engineering owing to their specific properties like non-toxicity, biodegradability and increased bone tissue growth [21]. The inhibitory effects of nHA as a calcium phosphate have been well documented in various cancer cells, such as liver [22], colon [23], gastric [24] and other [25] cancer cells. All the previous studies demonstrated that there were serious disagreements in inhibition degree of nHA on different types of cancer cell lines. As the structure of nHA and TCPNs are similar, the intrinsic anticancer characteristics of TCPNs are expected. Therefore, in this research, an *in vitro* model was developed to evaluate the inhibitory effects of TCPNs on MCF-7 breast carcinoma and G-292 osteosarcoma cell line response, as these had not been investigated before. In other words, for the first time, the inhibitory effect of TCPNs on breast cancer cells was studied (Fig. 2).

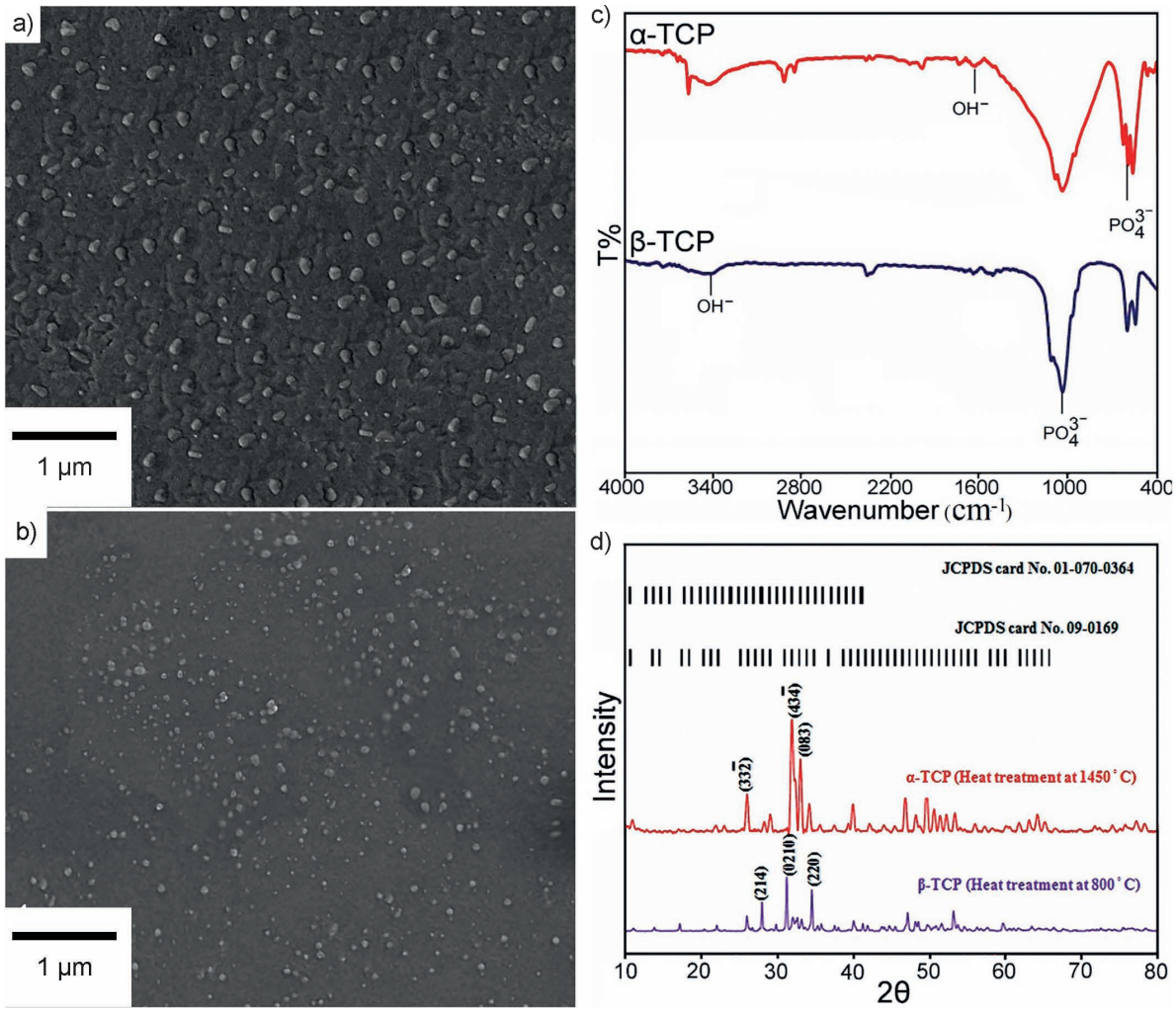


**Fig. 1:** SEM micrograph of TCP powders a) α-TCP, b) β-TCP, c) FT-IR spectra of the synthesized TCPNs after heat treatment, d) XRD patterns of the synthesized TCPNs after heat treatment at 800 °C and 1450 °C.

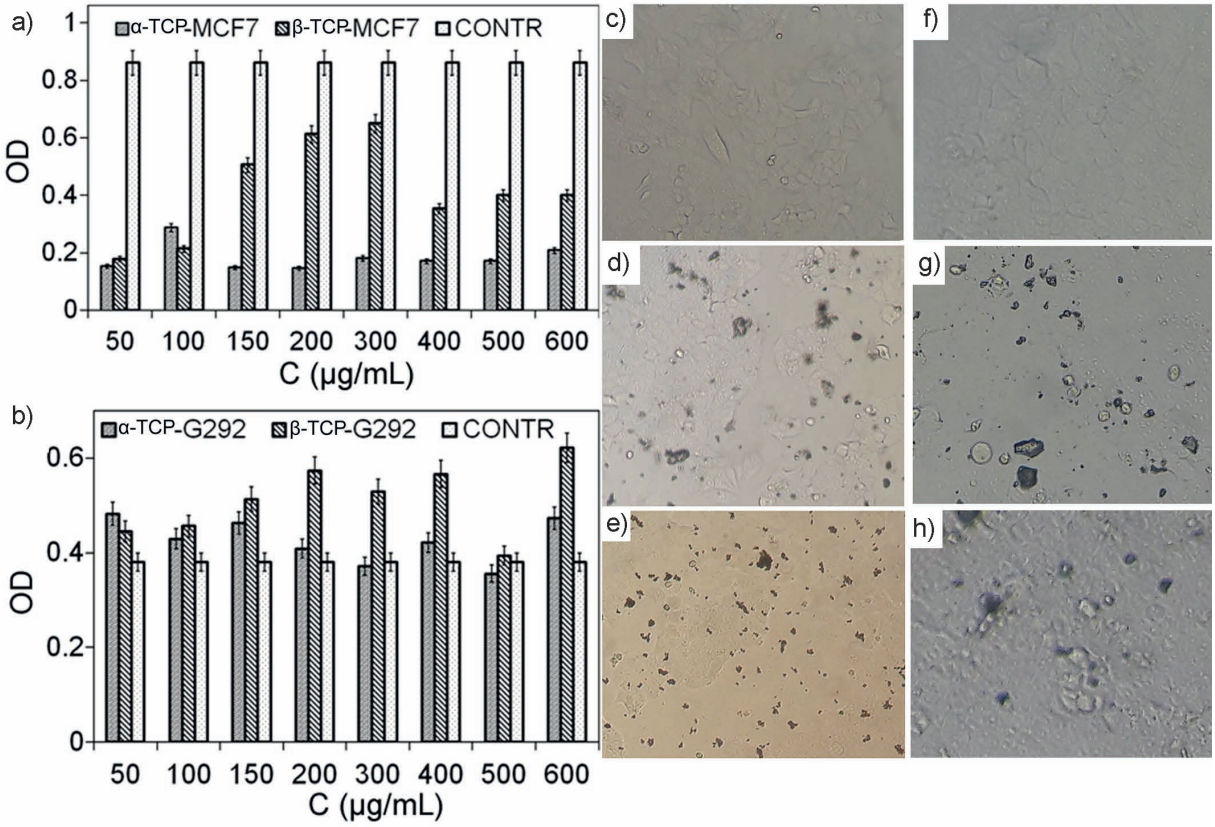


**Fig. 2:** The concentration effects of TCPNs on the proliferation of a) MCF-7 breast cancer cell, b) G-292 cells. c), d) and e) are cellular images of the control, 10 mg/L α-TCP and 200 mg/L β-TCP before 24-h cell culture (MCF-7) and f), g) and h) are cellular images of the control, 10 mg/L α-TCP and 200 mg/L β-TCP after 24 h cell culture (MCF-7).

It was reported that the new generation bisphosphonate ZA has demonstrated activity in the prevention of bone metastases [26]. It was known that a robust strategy to amplify the anti-cancer properties of TCPNs was ZA loading into TCP nanocarriers. *In vitro* release of ZA from both nanostructures (α and β-TCP) is depicted in Fig. 3. The properties of individual ZA depended on the two covalently bond side chains, named R1 and R2, attached to the central carbon atom as shown in Fig. 4 (a) [27]. It was proven that the third-generation bisphosphonates such as ZA had a direct antitumor effect, especially on osteoblast cells. Huang [28] *et al.* reported that ZA at the μM level affected osteoblast survival and migration, with no effect on the differentiation. It was found that ZA has direct effects on the proliferation and survival of osteoblast cells *in vitro*. For futher investigations about this drug delivery system, the effect of the bisphosphonate released from α and β-TCPNs on the growth inhibition of MCF-7, a breast cancer cell, is shown in Fig. 5. As expected, the time in ZA release system had affected the MCF-7 cell lines survival. Fig. 6 shows the influence of the drug released from TCP on the bone cell line.

## IV. Discussion

The scanning electron micrographs show that both synthesized TCPNs have a nanoscale and dense structure with well-dispersed particles. Fig. 1(a) in comparison with Fig. 1(b) indicates that the size of α-TCPNs calcined at higher temperature and for a longer time is larger than the β-TCP ones. The evaluations with more zoom in both structures demonstrated that the size of α-TCPNs was about 100 nm and its shape mostly spherical, the β-TCP particle size was nearly 70 nm. A similar ratio between the nanostructural size of α and β-TCP could be found in similar recent work [29].

In FTIR the additional broad bands at 1640 $cm^{-1}$ and 3430 $cm^{-1}$ formed owing to water adsorption. The bands at 568, 603 $cm^{-1}$ were obtained from the bending vibration of P-O mode; however, when the calcination temperature in α-TCP increased, the peaks merged. The 88 $cm^{-1}$ band was eventuated from the symmetric P-O stretching vibration in the $HPO_4^{-2}$ group that existed in non-stoichiometric HA. It was reported that the C-O vibration in the $CO_3^{-2}$ group could chip in this absorption band [20]. The strong bands at 1043 and 1093 $cm^{-1}$ were also related to the P-O stretching vibration of the $PO_4^{-3}$group. According to the FTIR figure, in the β-TCP and α-CP samples treated at 800 °C and 1450 °C, respectively, the OH absorption band disappeared and eventually the TCP spectrum formed. Finally, it could be said that the FT-IR spectrum of the β-TCP and α-TCP powders are similar, which was supported by further XRD results.

The phase evolution and grain size of the precipitated TCP precursors were evaluated with the XRD method. Fig. 1(d) shows the XRD analyses of the different synthesized TCP powders prepared with the precipitation method and sintered in air atmosphere at different temperatures of 800 °C and 1450 °C. According to the XRD results, as shown in Fig. 1(d), there are three distinct diffraction main peaks corresponding to the reflections of TCP polymorphs. The (0210), (220) and (214) peaks of the β-TCP related to the rhombohedral crystal system (JCPDS

Card File No. 09–0169) and (434), (083), (332) peaks of the α-TCP related to the monoclinic crystal system (JCPDS Card File No. 01–070–0364). It should be noted that this crystal system change could prove the phase evolution during β to α transformation during heat treatment. In other words, intense α-TCP peaks were perceived along with weak β-TCP peaks in the powder calcined at 1450 °C.

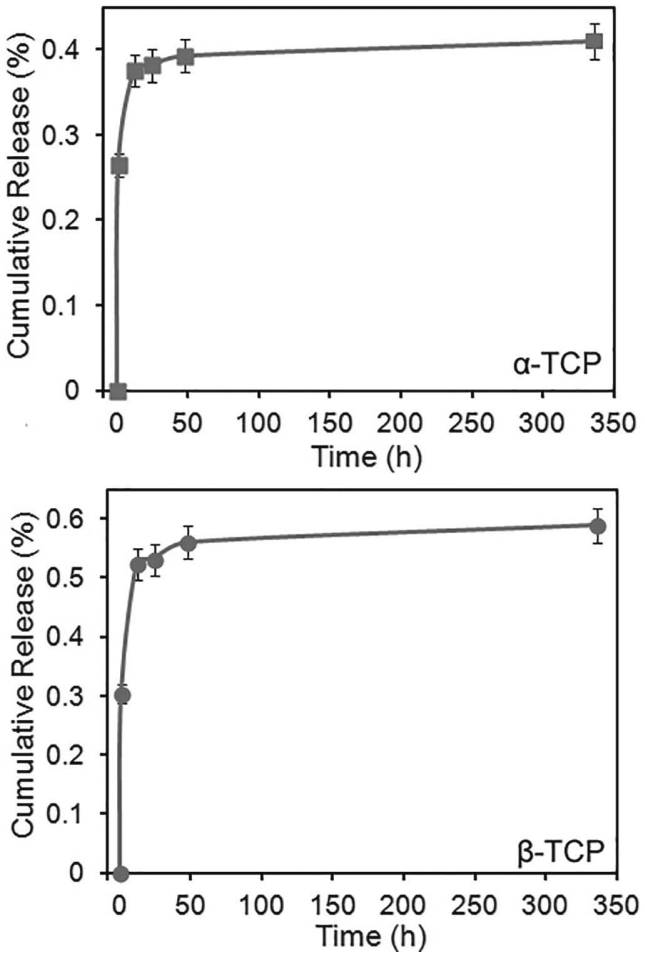


**Fig. 3:** Release profile of ZA (optimal dose, 0.08 g/L) loaded in TCPNs specimens.

For more information about the structure, the average nanocrystallite size was estimated from the half-width of three diffraction peaks, with the highest intensity, with the use of Debye Scherrer's equation as follows:

$$D = k\lambda/\beta \cos\theta \quad (1)$$

where D is the grain diameter, k is the shape factor (about 0.9), λ is the X-ray wavelength (1.5405 Å), β is the full width at half maximum (FWHM) of the diffraction line, and θ is the X-ray diffraction angle. Estimates obtained from the above equation indicated that the synthesized β-TCP and α-TCP crystallite sizes were nearly 25 and 38 nm, respectively. It was emphasized in previous works [30, 31] that Debye Scherrer's equation only gives an estimate of the crystallite average size. It should be noted that structural disorders and strain phenomena could lead to a peak broadening, which affects crystallite size evaluation. Therefore, it seems that the calculated values from XRD should be used mainly for comparison among the specimens. On the other hand, Choi *et al.* [31] justified the difference between the XRD and SEM results with reference to the highly agglomerated nature of the TCP nano-crystallites. He also reported that the heat treatment at higher temperatures indicated a slight growth of the clusters. Furthermore, the entire XRD and SEM results agreed that the powder size of the β-TCP was smaller than that of the α-TCP.

From Fig. 2, it is clear that the inhibitory effects of TCP-Ns on breast cancer cell proliferation were more effective than the control. The results showed that the differences in the inhibition effects of cancer cell proliferation among different concentrations were between 31 % to 90 % depending on the applied dosage. Morphology, particle size, and the dosage-dependent inhibitory effects of some calcium phosphates on cancer cells had also been proven previously in certain literature [22, 32–34]. It was reported that the sizes, morphologies, and concentrations of nano-HAP had significant effects on the apoptotic level.

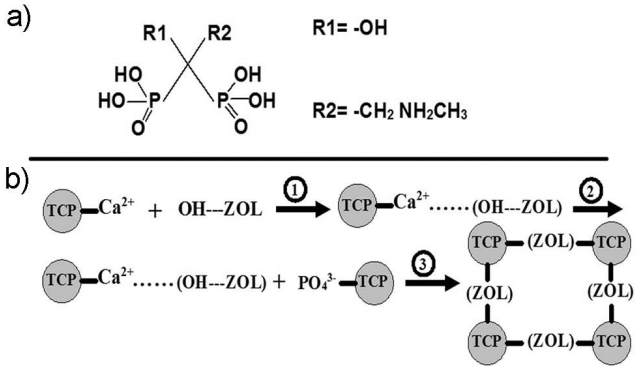


**Fig. 4:** Schematic representation of a) molecular structure of ZA, and b) the mechanism of chemical bonding between TCPNs and ZA.

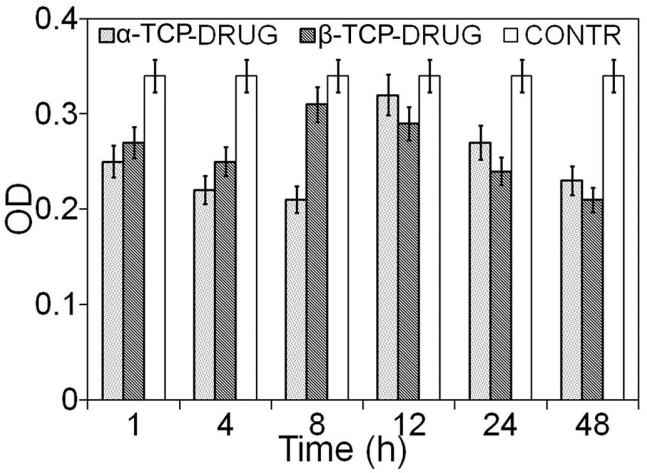


**Fig. 5:** Time-dependent ZA released from TCP carriers on MCF-7 proliferation.

According to the MTT results, at the concentration of 200 mg/L, the inhibitory effect of α-TCP particles on MCF-7 cells was significantly increased to about 83 % and further dosage enhancement was useless (Fig. 2(g)). Fig. 2(a) also showed that the inhibitory effects of α-TCP particles were independent of dosage. On the other hand, the inhibitory effect of β-TCPNs was reduced from 61 % (Fig. 2(a) and (h)) to about 25 % with dosage enhancement

(from 50 to 300 mg/L) and further increase up to 600 mg/l had no significant effect on results. These interesting results should be assessed in more detail in future work. An MTT assay was also performed to investigate the effect of β-TCPNs and α-TCPNs on bone cell line (G292) proliferation. According to the results shown in Fig. 2(b), β-TCPNs and α-TCPNs were biocompatible and increased cell proliferation; however, the results were independent of dosage for both materials. Therefore, these results demonstrated that β-TCPNs and α-TCPNs exhibit anticancer activity on breast cancer tumor cells and a non-toxic effect on normal cells. It should be mentioned that nanostructures like TCPNs could internalize into cancer cells through endocytic pathways [35] and reach the cytoplasm and different organelles that depend on their different characteristics and the final results of this work might be affected by this phenomenon.

Fast release of the drug in both nanocarriers could be perceived after 24 h, which indicated that the 80 %W of ZA was released from TCP nanocarriers after one day. It is clear that diffusion phenomena should be considered in drug release investigations. In this respect, it seems that the hydrophobic nature of nanostructures resulted in slow penetration of the sustained release into the medium and consequently, the slow release of the drug from both nanostructures. It should be mentioned here is that these nanostructures had a strong bond with the drug based on covalent bonds. To scrutinize this more closely, Fig. 4(a) shows the chemical structure of ZA. The two phosphonate groups are both essential for bonding to the bone mineral phase as well as cell-mediated antiresorptive activity. R1 substituents have prepared an additional capability in coordinating calcium, for example, hydroxyl (OH) or amino ($NH_2$) groups have provided a strong chemical bond with mineral materials, most likely via tridentate bonding to calcium. The R2 side group predominantly determines the antiresorptive potency of the bisphosphonates. In simple words, the presence of nitrogen atoms in the R2 side group is associated with the ability of an individual bisphosphonate to inhibit cell growth. Moreover, this point could affect bone affinity, as a function of the nitrogen moiety ability, in bonding with the surface of the bone mineral. It is shown in Fig. 4(b) that the chemical bonding between the TCPNs and ZA comprises three major steps described as follows: (1) A critical complex reaction between $Ca^{2+}$ ions of TCPNs and the OH group of the ZA. (2) The complex of $Ca^{2+}$ ions and ZA molecules assembled with $PO_4^{3-}$ ions. (3) P-O and O-H groups of TCPNs form chemical bonds with the -OH and -$NH_2$ groups in the ZA molecule, resulting in ZA drug layers that were strongly attached to the surface of TCPNs as shown schematically in Fig. 4(b). Therefore, according to the initial results, it seems expedient to design an implantable bisphosphonate delivery system for ZA based on these α and β-TCP nanostructures.

The main results of Fig. 5 showed that cell survival decreased after 1 h, demonstrating that the cells were suffering from drug overdose (Fig. 4). According to Fig. 6, there was an equivalent point in survival after 12 h and additional time had no effect on G292 cell viability. However, in comparison with Fig. 5 for MCF-7 cells, the viability dependence on the time for the MCF-7 cells was more visible than for G292 cells in both α and β-TCP nanostructures. The results in Fig. 6 indicate that the treatment of MCF-7 breast cancer cells with the ZA reduced cell viability during different times, to put it simply, these drug delivery systems could be used in breast cancer treatment. Also, as shown in Figs. 5 and 6, the combination of α and β-TCP with ZA did not significantly augment apoptosis in any of the G292 or MCF-7 cell lines. These observations suggest that loaded ZA in TCPNs like α and β-TCP could be used in bone and breast cancer treatment. However, it is suggested that further investigations into this drug delivery system should be undertaken.

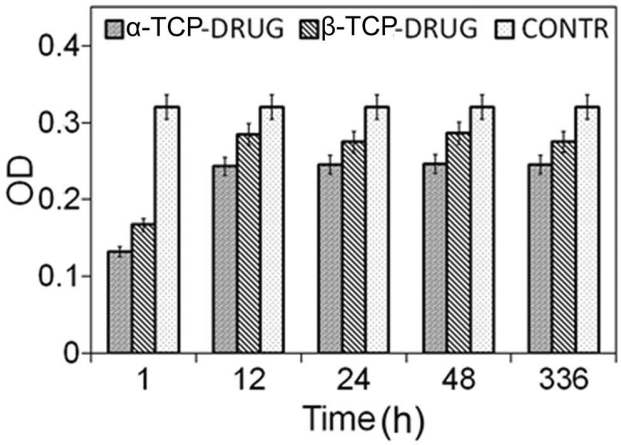


**Fig. 6:** Time-dependent ZA released from TCP carriers on G-292 cell proliferation.

## V. Conclusions

In brief, structures, chemical properties and the inhibitory effect of TCPNs as a carrier for the release of the ZA on MCF-7 breast cancer and G-292 osteosarcoma cell lines were investigated. The main results are summarized as follows:

1. The structural characterization of the both α and β-TCP in nanoscale was investigated by means of SEM and XRD analysis. The SEM analysis of the microstructure indicated a dense structure with well-dispersed particles for all specimens. The SEM and XRD results supported that particle size of the synthesized α and β-TCP were below 100 nm with spherical shapes and the β-TCP particle size was smaller than that of α-TCP.
2. The FT-IR spectrum comparison between β-TCP and α-TCP powders besides the crystal system change in XRD peaks confirmed the phase evolution during β to α transformation in heat treatment.
3. Inhibitory effects of TCPNs on the growth and proliferation of MCF-7 breast cancer and G-292 osteosarcoma cell lines were investigated *in vitro* tests. From the results obtained, it could be concluded that TCPNs induced oxidative stress to the breast cancer cells which led to apoptotic-like conditions. In other words, TCPNs could inhibit the proliferation of human cancer cells.

4. According to the MTT assay, β-TCPNs and α-TCPNs were biocompatible and the inhibitory effects of β-TCPNs and α-TCPNs on both MCF-7 and G-292 cells were independent of their dosage. The best inhibitory effect (83 %) was assigned to α-TCPNs with a concentration of 200 mg/L on MCF-7 cells.
5. A fast release was seen in both nanocarriers, which indicated that 80 %W of ZA was released from TCP carriers after one day. However, these nanostructures had strong covalent bonds with the drug.
6. The time in the ZA release system affected the G292 or MCF-7 cell line survival and the viability dependence on time for the MCF-7 cells was more visible than for G292 cells in both α and β-TCP nanostructures.

TCPNs as carriers could regulate the release of ZA to inhibit cancer cell proliferation. Therefore, in consideration of these satisfactory results, it is hoped that these drug delivery systems (loaded ZA in TCPNs) could be used in future bone and breast cancer treatments.

## References


1 Weigelt, B., Peterse, J.L., Van't Veer, L.J.: Breast cancer metastasis: Markers and models, *Nat. Rev. Cancer*, **5**, 591 – 602, (2005).

2 Joyce, J.A., Pollard, J.W.: Microenvironmental regulation of metastasis, *Nat. Rev. Cancer*, **9**, 239 – 252, (2009).

3 Clemons, M., Gelmon, K., Pritchard, K., Paterson, A.: Bone-targeted agents and skeletal-related events in breast cancer patients with bone metastases: The state of the art, *Curr. Oncol.,* **19**, 259 – 268, (2012).

4 Frede, A., Neuhaus, B., Klopfleisch, R., Walker, C., Buer, J., Müller, W., Epple, M., Westendorf, A.M.: Colonic gene silencing using siRNA-loaded calcium phosphate/PLGA nanoparticles ameliorates intestinal inflammation in vivo, *J. Control. Release,* **222**, 86 – 96, (2016).

5 Gao, X., Lan, J., Jia, X., Cai, Q., Yang, X.: Improving interfacial adhesion with epoxy matrix using hybridized carbon nanofibers containing calcium phosphate nanoparticles for bone repairing, *Mater. Sci. Eng. C.,* **61**, 174 – 179, (2016).

6 Karimi, M., Hesaraki, S., Alizadeh, M., Kazemzadeh, A.: Synthesis of calcium phosphate nanoparticles in deep-eutectic choline chloride-urea medium: Investigating the role of synthesis temperature on phase characteristics and physical properties, *Ceram. Int.,* **42**, 2780 – 2788, (2016).

7 Qian, J., Ma, J., Su, J., Yan, Y., Li, H., Shin, J.-W., Wei, J., Zhao, L.: PHBV-based ternary composite by intermixing of magnesium calcium phosphate nanoparticles and zein: In vitro bioactivity, degradability and cytocompatibility, *Eur. Polym. J.,* **75**, 291 – 302, (2016).

8 Zhang, J., Sun, X., Shao, R., Liang, W., Gao, J., Chen, J.: Polycation liposomes combined with calcium phosphate nanoparticles as a non-viral carrier for siRNA delivery, *J. Drug Deliv. Sci. Technol.,* **30**, 1 – 6, (2015).

9 Mi, P., Kokuryo, D., Cabral, H., Kumagai, M., Nomoto, T., Aoki, I., Terada, Y., Kishimura, A., Nishiyama, N., Kataoka, K.: Hydrothermally synthesized PEGylated calcium phosphate nanoparticles incorporating Gd-DTPA for contrast enhanced MRI diagnosis of solid tumors, *J. Control. Release,* **174**, 63 – 71, (2014).

10 Koshkaki, M.R., Ghassai, H., Khavandi, A., Seyfoori, A., Molazemhosseini, A.: Effects of formaldehyde solution and nanoparticles on mechanical properties and biodegradation of gelatin/nano β-TCP scaffolds, *Iran. Polym. J.,* **22**, 653 – 664, (2013).

11 Zekri, J., Mansour, M., Karim, S.M.: The anti-tumour effects of zoledronic acid, *J. Bone. Oncol.,* **3**, 25 – 35, (2014).

12 Mitri, Z., Nanda, R., Blackwell, K., Costelloe, C.M., Hood, I., Wei, C., Brewster, A.M., Ibrahim, N.K., Koenig, K.B., Hortobagyi, G.N.: TBCRC-010: Phase I/II study of dasatinib in combination with zoledronic acid for the treatment of breast cancer bone metastasis, *Clin. Cancer Res.,* **22**, 5706 – 5712, (2016).

13 Bose, S., Tarafder, S.: Calcium phosphate ceramic systems in growth factor and drug delivery for bone tissue engineering: a review, *Acta. Biomater.,* **8**, 1401 – 1421, (2012).

14 Barrère, F., van Blitterswijk, C.A., de Groot, K.: Bone regeneration: molecular and cellular interactions with calcium phosphate ceramics, *Int. J. Nanomedicine,* **1**, 317 – 332, (2006).

15 Ottewell, P.D., Mönkkönen, H., Jones, M., Lefley, D.V., Coleman, R.E., Holen, I.: Antitumor effects of doxorubicin followed by zoledronic acid in a mouse model of breast cancer, *J. Natl. Cancer Inst.,* **100**, 1167 – 1178, (2008).

16 Brufsky, A.M., Bosserman, L.D., Caradonna, R.R., Haley, B.B., Jones, C.M., Moore, H.C., Jin, L., Warsi, G.M., Ericson, S.G., Perez, E.A.: Zoledronic acid effectively prevents aromatase inhibitor-associated bone loss in postmenopausal women with early breast cancer receiving adjuvant letrozole: Z-FAST study 36-month follow-up results, *Clin. Breast Cancer,* **9**, 77 – 85, (2009).

17 Meena, R., Kesari, K.K., Rani, M., Paulraj, R.: Effects of hydroxyapatite nanoparticles on proliferation and apoptosis of human breast cancer cells (MCF-7), *J. Nanopart. Res.,* **14**, 1 – 11, (2012).

18 Han, Y., Li, S., Cao, X., Yuan, L., Wang, Y., Yin, Y., Qiu, T., Dai, H., Wang, X.: Different inhibitory effect and mechanism of hydroxyapatite nanoparticles on normal cells and cancer cells *in vitro* and *in vivo*, *Sci. Rep.,* **4**, 7134 – 7140, (2014).

19 Liu, J., Zhao, L., Ni, L., Qiao, C., Li, D., Sun, H., Zhang, Z.: The effect of synthetic α-tricalcium phosphate on osteogenic differentiation of rat bone mesenchymal stem cells, *Am. J. Transl. Res.,* **7**, 1588 – 1601, (2015).

20 Kwon, S.-H., Jun, Y.-K., Hong, S.-H., Kim, H.-E.: Synthesis and dissolution behavior of β-TCP and HA/β-TCP composite powders, *J. Eur. Ceram. Soc.,* **23**, 1039 – 1045, (2003).

21 Erisken, C., Kalyon, D.M., Wang, H.: Functionally graded electrospun polycaprolactone and β-tricalcium phosphate nanocomposites for tissue engineering applications, *Biomaterials*, **29**, 4065 – 4073, (2008).

22 Yuan, Y., Liu, C., Qian, J., Wang, J., Zhang, Y.: Size-mediated cytotoxicity and apoptosis of hydroxyapatite nanoparticles in human hepatoma HepG2 cells, *Biomaterials*, **31**, 730 – 740, (2010).

23 Venkatesan, P., Puvvada, N., Dash, R., Kumar, B.P., Sarkar, D., Azab, B., Pathak, A., Kundu, S.C., Fisher, P.B., Mandal, M.: The potential of celecoxib-loaded hydroxyapatite-chitosan nanocomposite for the treatment of colon cancer, *Biomaterials*, **32**, 3794 – 3806, (2011).

24 Li, J., Yin, Y., Yao, F., Zhang, L., Yao, K.: Effect of nano- and micro-hydroxyapatite/chitosan-gelatin network film on human gastric cancer cells, *Mater. Lett.*, **62**, 3220 – 3223, (2008).

25 Tang, W., Yuan, Y., Liu, C., Wu, Y., Lu, X., Qian, J.: Differential cytotoxicity and particle action of hydroxyapatite nanoparticles in human cancer cells, *Nanomedicine*, **9**, 397 – 412, (2014).

26 Gu, W., Wu, C., Chen, J., Xiao, Y.: Nanotechnology in the targeted drug delivery for bone diseases and bone regeneration, *Int. J. Nanomedicine*, **8**, 2305 – 2317, (2013).

27 Heymann, D.: Zoledronic Acid, Encyclopedia of Cancer, Springer, Berlin Heidelberg, 2011.

28 Huang, K.-C., Cheng, C.-C., Chuang, P.-Y., Yang, T.-Y.: The effects of zoledronate on the survival and function of human

osteoblast-like cells, *BMC. Musculoskelet. Disord.*, **16**, 355, (2015).

[29] Gallinetti, S., Canal, C., Ginebra, M.P.: Development and characterization of biphasic hydroxyapatite/β-TCP cements, *J. Am. Ceram. Soc.*, **97**, 1065 – 1073, (2014).

[30] Tadic, D., Epple, M.: A thorough physicochemical characterisation of 14 calcium phosphate-based bone substitution materials in comparison to natural bone, *Biomaterials.*, **25**, 987 – 994, (2004).

[31] Choi, D., Kumta, P.N.: Mechano-chemical synthesis and characterization of nanostructured β-TCP powder, *Mater. Sci. Eng. C.*, **27**, 377 – 381, (2007).

[32] Xu, Z., Liu, C., Wei, J., Sun, J.: Effects of four types of hydroxyapatite nanoparticles with different nanocrystal morphologies and sizes on apoptosis in rat osteoblasts, *J. Appl. Toxicol.*, **32**, 429 – 435, (2012).

[33] Rahmanian, M., Naghib, S.M., Seyfoori, A., Zare, A.A., Sanati, H., Majidzadeh-A, K.: Inhibitory effect of tricalcium phosphate sintered at different temperatures on human breast cancer cell line MCF-7, *Multidiscip. Cancer. Invest.,* **1**, 11 – 14, (2016).

[34] Rahmanian, M., Naghib, M., Seyfoori, A., Zare, A.A., Majidzadeh-A, K.: Investigation of inhibitory effect of β-tricalcium phosphate on MCF-7 Proliferation. iranian journal of breast disease, *Iran. J. Breast. Dis.*, **9**, 7 – 13, (2016).

[35] Chen, T., Shukoor, M.I., Wang, R., Zhao, Z., Yuan, Q., Bamrungsap, S., Xiong, X., Tan, W.: Smart multifunctional nanostructure for targeted cancer chemotherapy and magnetic resonance imaging, *ACS. Nano.*, **5**, 7866 – 7873, (2011).